



Preparation, coordination properties and catalytic use of 1'-(diphenylphosphanyl)-1-ferrocenecarboxamides bearing 2-hydroxyethyl pendant groups

Jiří Schulz, Ivana Čísařová, Petr Štěpnička *

Department of Inorganic Chemistry, Faculty of Science, Charles University, Hlavova 2030, 12840 Prague, Czech Republic

ARTICLE INFO

Article history:

Received 14 February 2009

Received in revised form 30 March 2009

Accepted 8 April 2009

Available online 17 April 2009

Keywords:

Ferrocene

Phosphanyl-carboxamides

Palladium

Suzuki–Miyaura reaction

Water-soluble ligands

Structure elucidation

ABSTRACT

Polar amido-phosphane ligands, viz 1-(diphenylphosphanyl)-1'-[N-(2-hydroxyethyl)carbamoyl]ferrocene (**1**) and 1-(diphenylphosphanyl)-1'-[N,N-bis(2-hydroxyethyl)carbamoyl]ferrocene (**2**) were synthesised from 1'-(diphenylphosphanyl)-1-ferrocenecarboxylic acid (Hdpf) by direct amide coupling or via Hdpf-pentafluorophenyl ester **3**. Subsequent reactions of **1** and **2** with [PdCl₂(cod)] (cod = η²:η²-cycloocta-1,5-diene) gave the respective bis(phosphane) complexes *trans*-[PdCl₂L₂] (**4**, L = **1**; **5**, L = **2**). Depending on the solvent used in their subsequent crystallisation (ethanol or chloroform), these complexes were isolated in several defined solvated forms. The structure determination for free ligands and their solvated complexes (**4**·2EtOH, **4**·6CHCl₃, **5**·2EtOH, and **5**·4CHCl₃) revealed the dominating role of hydrogen bonding in their crystal assemblies, the nature and complexity of the formed hydrogen-bonded arrays strongly varying with the ligand structure (one vs. two 2-hydroxyethyl chains), their number in the discrete species (free ligands vs. the complexes), and also with the solvate. Catalytic tests performed with **4** and **5** in Suzuki–Miyaura cross-coupling reaction showed that both complexes form active catalysts for the coupling of aryl bromides with phenylboronic acid in common polar organic solvents, in water and in toluene–water biphasic mixture. Yet, complex **4** gave rise to hydrolytically more stable catalyst, which could be used five times without any detectable loss of activity in the toluene/water system. Complex **4** was also successfully applied to the synthesis of biaryl anti-inflammatory drugs and their analogues in pure water and in the toluene–water mixture.

© 2009 Elsevier B.V. All rights reserved.

1. Introduction

Ferrocene ligands have found manifold use as catalyst components for various transition metal-mediated reactions [1,2]. Despite their vast number, there is continuing demand for new ferrocene donors, particularly those tailored for a specific reaction type, substrate and reaction solvent. The ligand design thus reflects the surge for the development of “green” synthetic processes based on alternative feedstock and environmentally benign solvents including water and homogeneous or biphasic water–organic solvent mixtures [3,4]. The application of ferrocene phosphanes, that are the most abundant and successful class among the ferrocene donors [1,2], is unfortunately hindered in aqueous media by their hydrophobic nature. Attempts to prepare water-soluble ferrocene phosphanes for *catalytic* use remain still very scarce and can be demonstrated by the synthesis of a chiral ferrocene diphosphane modified with a hydrophilic urea tag [5].

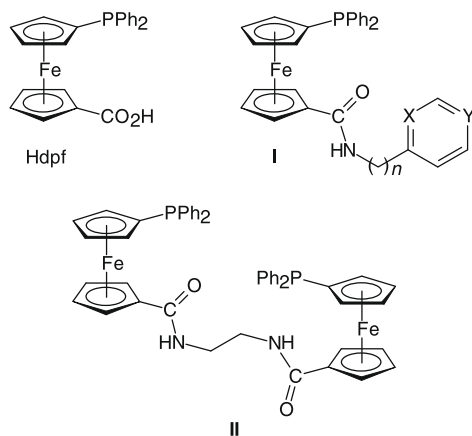
While studying phosphanyl-ferrocenecarboxylic acids [6,7], we found that introduction of a single CO₂H group already improves

water-solubility of (diphenylphosphanyl)ferrocene moiety, particularly when the group is dissociated [8]. In order to prepare ferrocene ligands with a higher affinity to water and aqueous media in their native (non-dissociated) form, we decided to make use of the synthetic potential of the carboxyl group rather than its inherent polarity. Among carboxylic derivatives, we chose amides that are resistant towards hydrolysis (particularly ferrocene ones) and can be structurally varied through changing the substituents at the amide nitrogen.

Recently, we reported about the preparation of phosphanyl-ferrocene-carboxamides from 1'-(diphenylphosphanyl)ferrocene-1-carboxylic acid (Hdpf; Scheme 1) [8a] and their utilisation as synthetic precursors to chiral ferrocene oxazolines [9] and P-chelated carbenes [10], and as ligands for transition metals and metal-catalysed reactions (Scheme 1, I: *n* = 1, X/Y = N/CH, CH/N; *n* = 2, X/Y = N/CH [11]; II and PAMAM-analogues [12]). Furthermore, we designed several types of chiral phosphanylferrocene-carboxamides, that proved to be efficient ligands for palladium-catalysed asymmetric allylic alkylation [7b,13]. This contribution extends our previous studies on phosphanyl-ferrocene carboxamides, dealing with the synthesis of novel Hdpf-based amides bearing the 2-hydroxyethyl groups at the amide nitrogen. Preparation of

* Corresponding author. Fax: +420 221 951 253.

E-mail address: stepnic@natur.cuni.cz (P. Štěpnička).



Scheme 1.

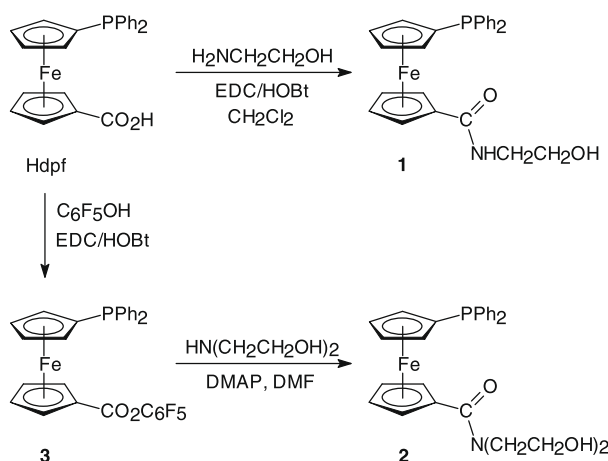
palladium(II) complexes from these ligands and their use in palladium-catalysed Suzuki–Miyaura cross-coupling in homogeneous and biphasic polar reaction media are also reported.

2. Results and discussion

2.1. Preparation and crystal structures of the ligands

1-(Diphenylphosphanyl)-1'-[N-(2-hydroxyethyl)carbamoyl]ferrocene (**1**) and 1-(diphenylphosphanyl)-1'-[N,N-bis(2-hydroxyethyl)carbamoyl]ferrocene (**2**) were both prepared from Hdpf (Scheme 2). Whereas the former compound resulted directly by reaction of Hdpf with 2-aminoethanol in the presence of peptide coupling agents [14], a similar reaction with diethanolamine afforded only unreacted Hdpf-benzotriazolyl ester [12a]. Hence, the desired tertiary amide **2** was synthesised alternatively via active Hdpf-pentafluorophenyl ester (**3**) [15]. The amides were isolated by column chromatography and further purified by crystallisation from ethyl acetate–hexane to afford analytically pure **1** and **2** as air-stable orange crystalline solids in 82% and 70% yield, respectively.

In IR spectra, compounds **1** and **2** display diagnostic $\nu_{\text{C=O}}$ (amide I) bands at 1633 and 1594 cm^{-1} , respectively. For **1**, an additional $\delta_{\text{N-H}}$ band (amide II) is seen at 1552 cm^{-1} . ^1H and ^{13}C NMR spectra support the formulations by showing characteristic



Scheme 2. Preparation of **1** and **2** (EDC, *N*-[3-dimethylamino]propyl-*N'*-ethylcarbodiimide; HOBt, 1-hydroxybenzotriazole; DMF, *N,N*-dimethylformamide; DMAP, 4-(dimethylamino)pyridine).

sets of signals due to the phosphanoferrocenyl and the amide moieties. The spectra of secondary amide **1** reveal no unexpected features at room temperature (in CDCl_3) whilst those of **2** show markedly broadened resonances of the amide pendants. Such signal broadening apparently reflects a limited mobility of the polar chains, resulting from their hydrogen bonding interactions. Variable-temperature (VT) NMR spectra support this explanation (Fig. 1). The ^1H NMR spectrum of **2** recorded at 50 °C displays the signals due to the ethan-1,2-diyl groups as a pair of triplets as expected for the equivalent 2-hydroxyethyl chains that are void of mobility constraints and rapidly exchange the acidic hydrogens. Upon cooling, the exchange processes become slower, which is reflected first by broadening of the signals and then by separation of four distinct resonances. Further cooling to –25 °C causes a collapse of two neighbouring signals into a broad singlet. The $^{31}\text{P}\{^1\text{H}\}$ NMR signals of **1** and **2** are found at positions similar to that of free Hdpf [8a].

The molecular structures of **1** and **2** are shown in Figs. 2 and 3 together with selected geometric data. In both compounds, the geometry of ferrocene moieties are quite regular with similar Fe–ring centroid (Cg) distances and tilts below 5°. As evidenced by the torsion angles C1–Cg1–Cg2–C6 = 93° for **1** and 83° for **2** (see Fig. 2 for definitions), the ferrocene substituents are mutually rotated, adopting intermediate conformations between synclinal-eclipsed and anticlinal-staggered. The amide moieties are planar [cf. the torsion angles O1–C1–N–C24 = 8.5(3)° for **1**, and O1–C1–N–C24/O1–C1–N–C26 = 175.1(1)/2.8(2)° for **2**] but deviate from the planes of their parent rings Cp1 [cf. the dihedral angles of the {C11O1N} and Cp1 planes: 18.5(2)° in **1** and 18.3(3)° in **2**].

In the solid state, the molecules of **1** and **2** associate expectedly by means of hydrogen-bond interactions generated by their polar amide pendants. The molecules of **1** assemble into inversion-related pairs via hydrogen bonds between the terminal hydroxyl and the amide carbonyl groups, O2–H92...O1 (Fig. 4 and Table 1). These pairs are further connected by N–H91...O2 hydrogen bonds to four adjacent molecules so that each dimer unit acts as a twofold hydrogen bond donor and a twofold acceptor. When combined, such interactions result in the formation of infinite layers oriented parallel to the crystallographic *ac* plane (at $y = 0, \frac{1}{2},$ and 1 in the unit cell). The bulky non-polar phosphanoferrocenyl moieties are

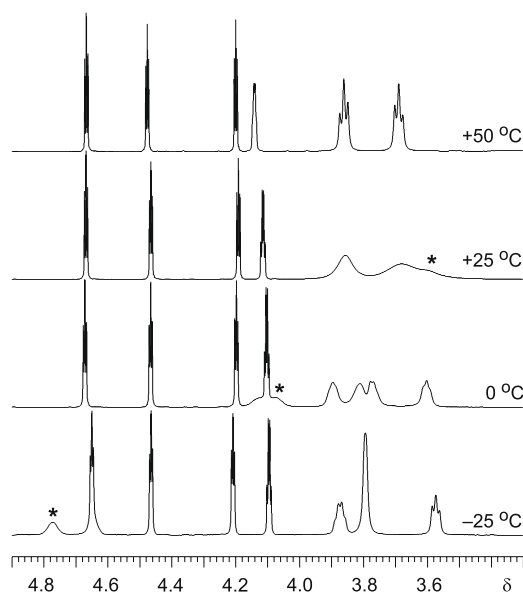


Fig. 1. VT ^1H NMR spectra of amide **2** in the region of ferrocene (CH) and aliphatic (CH_2) protons. The asterisk indicates the signal due to hydrogen-bonded protons whose position changes with the temperature.

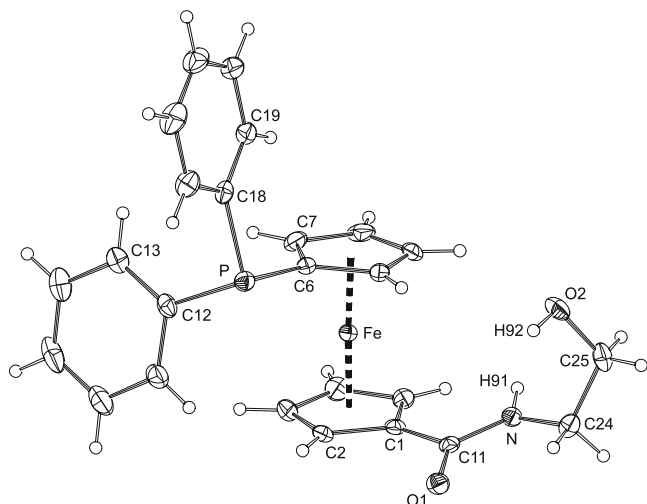


Fig. 2. View of the molecular structure of **1** showing displacement ellipsoids at the 30% probability level. Selected distances and angles (Å and °): Fe–Cg1 1.6510(9), Fe–Cg2 1.644(1), C1–C11 1.476(2), C11–O1 1.240(2), C11–N 1.340(2), N–C24 1.448(2), C25–O2 1.418(2), P–C6 1.810(2), P–C12 1.838(2), P–C18 1.839(2); <Cp1,Cp2 4.5(1), O1–C11–N 122.2(2), C11–N–C24 123.1(2), C24–C25–O2 114.3(2). The ring planes are defined as follows: Cp1 = C(1–5), Cp2 = C(6–10), Ph1 = C(12–17), Ph2 = C(18–23); Cg1 and Cg2 stand for the centroids of the rings Cp1 and Cp2, respectively.

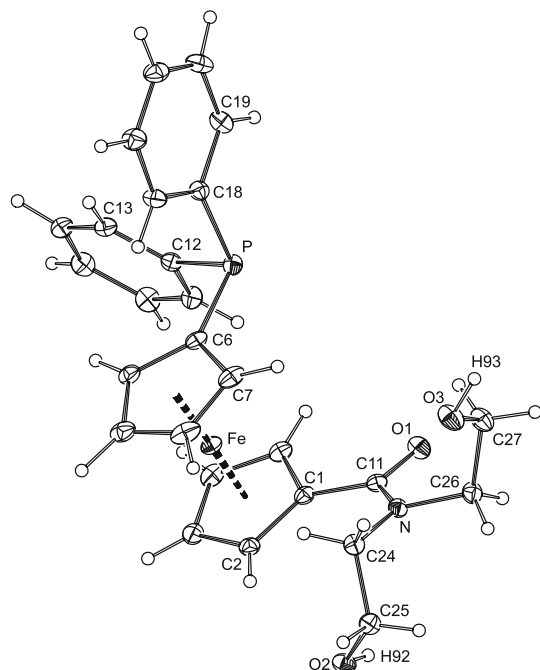


Fig. 3. Thermal ellipsoid plot of **2**, drawn at the 30% probability level. Selected distances and angles (Å and °): Fe–Cg1 1.6558(8), Fe–Cg2 1.6467(9), C1–C11 1.494(2), C11–O1 1.244(2), C11–N 1.351(2), N–C24 1.468(2), N–C26 1.479(2), C25–O2 1.423(2), C26–O3 1.426(2), P–C(6) 1.819(2), P–C12 1.844(2), P–C18 1.837(2); <Cp1,Cp2 0.7(1), O1–C11–N 119.5(2), C11–N–C24 127.4(2), C11–N–C26 116.6(1), C24–C25–O2 113.3(1), C26–C27–O3 109.8(1). The ring planes are defined as for **1**.

packed essentially at the distances defined by their van der Waals envelope and thus separate the polar hydrogen-bonded sheets.

Similarly to **1**, the molecules of **2** form centrosymmetric dimers via pairs of hydrogen bonds between the hydroxyl and carbonyl groups, O2–H92...O1 (Fig. 5 and Table 1). However, in contrast to **1**, the dimers in the crystals of **2** further associate in only one dimension forming infinite ribbons via hydrogen bonds between the hydroxyl group of the ‘other’ hydroxyethyl chain and the OH oxygen in an adjacent dimer unit.

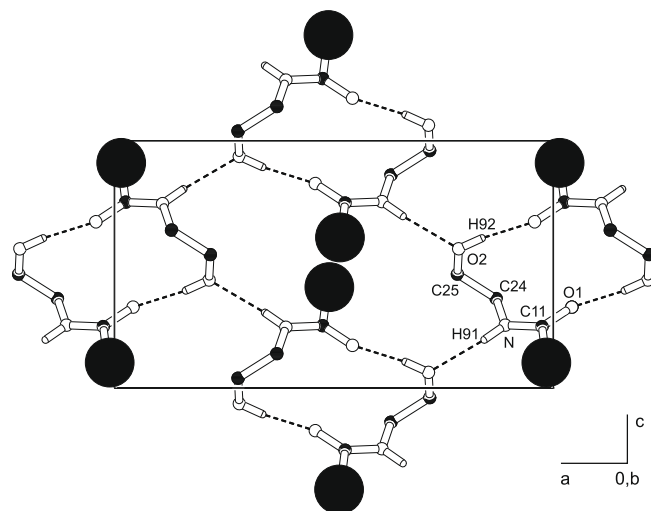


Fig. 4. A projection of a hydrogen-bonded layer in solid **1** onto the *ac* plane (at $b = 0$). Because of the crystallographic symmetry, the layer located at $b/2$ is shifted by $c/2$. Hydrogen bonds are shown as dashed lines and the 1'-(diphenylphosphanyl)ferrocen-1-yl moieties were replaced with black circles.

Table 1
Summary of hydrogen bond parameters.^a

D–H...A	D...A (Å)	Angle at H (°)
Compound 1		
O2–H92...O1 ⁱ	2.666(2)	167
N–H92...O2 ⁱⁱ	2.955(2)	153
Compound 2		
O2–H92...O1 ⁱⁱⁱ	2.691(2)	170
O3–H93...O2 ^{iv}	2.833(2)	165
Compound 4·2EtOH		
N–H91...O2 ^v	2.934(3)	163
O2–H92...O3	2.714(4)	173
O3–H93...O1 ^{vi}	2.674(5)	168
Compound 4·6CHCl₃		
N–H91...O1 ^{vii}	3.311(4)	154
O2–H92...O1 ^{viii}	2.697(4)	166
C70–H70...O2 ^{ix}	3.089(5)	173
C80–H80...Cl	3.602(4)	144
Compound 5·2EtOH		
O2–H91...O3	2.740(2)	161
O3–H92...O4 ^x	2.641(3)	168
O4–H93...O1	2.617(3)	173
Compound 5·4CHCl₃		
O2–H91...O3 ^x	2.666(4)	164
O3–H92...O1 ^{xi}	2.660(4)	166
C80–H80...Cl ^{xii}	3.569(4)	144

^a D, donor; A, acceptor. Symmetry codes: *i.* $-x, -y, 1-z$; *ii.* $\frac{1}{2}-x, y, -\frac{1}{2}+z$; *iii.* $1-x, 2-y, -z$; *iv.* $1+x, y, z$; *v.* $2-x, 2-y, 1-z$; *vi.* $1+x, y, z$; *vii.* $3/2-x, 1/2+y, 1/2-z$; *viii.* $2-x, 1-y, 1-z$; *ix.* $1-x, 1-y, 1-z$; *x.* $2-x, -y, 1-z$; *xi.* $1-x, -y, -z$; *xii.* $1+x, y, z$. The solvent molecules are labelled as follows: C31–C30–O3–H93 for **4·2EtOH**, C31–C30–O4–H93 for **5·2EtOH**, C70–H70–Cl(71.72,73)/C80–H80–Cl(81.82,83)/C90–H90–Cl(91.92,93) for **4·6CHCl₃**, and C80–H80–Cl(81.82,83)/C90–H90–Cl(91.92,93) for **5·4CHCl₃**.

2.2. Preparation and crystal structures of palladium(II) complexes

Replacement of the diene ligand in [PdCl₂(cod)] (cod = η²:η²-cycloocta-1,5-diene) with the stoichiometric amounts of **1** and **2** expectedly gave the respective bis(phosphane) complexes **4** and **5** (Scheme 3). The complexes possess a strong tendency to retain reaction solvents but, fortunately, separate as defined stoichiometric solvates upon crystallisation. Depending on the solvent used (ethanol or CHCl₃), the following crystalline solvates were isolated

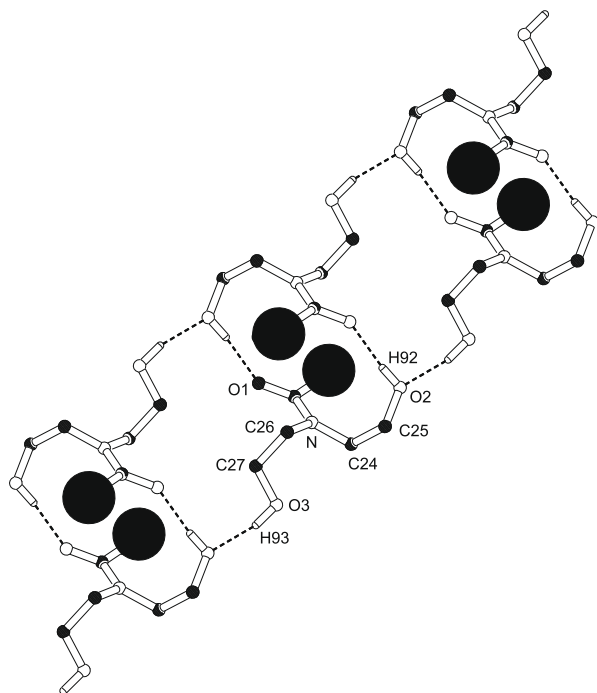
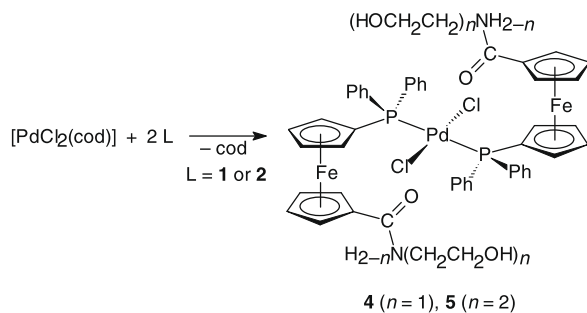


Fig. 5. Section of the ladder-like hydrogen-bonded array in the crystal of **2**. The hydrogen bonds are indicated with dashed lines and the phosphanoferrocenyl moieties were replaced with black circles.



Scheme 3. Preparation of complexes **4** and **5** (cod = cycloocta-1,5-diene).

and structurally characterised: **4**·2EtOH, **5**·2EtOH, **4**·6CHCl₃, and **5**·4CHCl₃.

Spectroscopic data for **4** and **5** suggest P-monodentate coordination of the ferrocene ligands. The amide bands in IR spectra are observed at positions similar to the free ligands while the ³¹P{¹H} NMR signals appear shifted to lower fields, to a position similar to *trans*-[PdCl₂(Hdpf-κP)₂] ($\delta_P +16.8$) [16]. The VT ¹H NMR spectra of the complexes do not show any unexpected features. The solid-state structures of **4**·2EtOH, **4**·6CHCl₃, **5**·2EtOH and **5**·4CHCl₃ have been established by single-crystal X-ray diffraction. Structures of the ethanol solvates are depicted in Figs. 6 and 7 (the structures of the complex moieties in the crystals of the CHCl₃ solvates are very similar). Selected geometric data for all solvatomorphs are presented in Table 2.

The structures confirm the expected *trans*-square planar geometry in all cases. The coordination environments around the palladium atoms show minor angular deformations—though without any pronounced tetrahedral distortion because of the imposed symmetry (the Pd atoms reside on the crystallographic inversion centres). The deviation of the interligand angles from 90° (by ca. ±5°) likely helps in minimising steric interaction of the ligands.

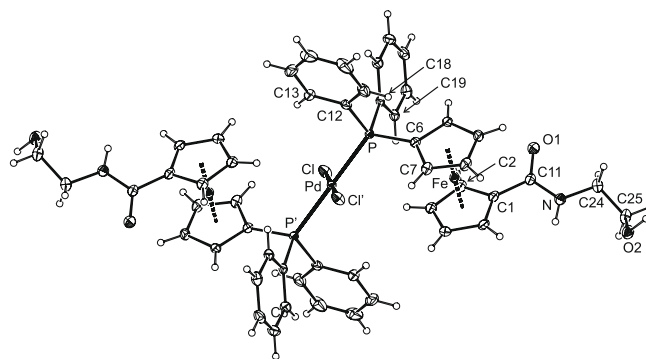


Fig. 6. View of the complex molecule in the structure of **4**·2EtOH. Displacement ellipsoids enclose the 30% probability level. The half of the molecule is generated by the inversion operation.

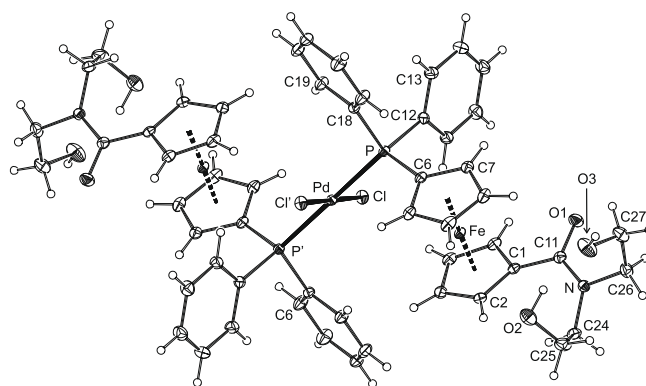


Fig. 7. View of the complex molecule in the structure of **5**·2EtOH showing displacement ellipsoids at the 30% probability level. The half of the molecule is generated by the inversion operation.

Table 2

Selected distances and angles for **4**·2EtOH, **4**·6CHCl₃, **5**·2EtOH and **5**·4CHCl₃ (Å, °).^a

Parameter	4 ·2EtOH	4 ·6CHCl ₃	5 ·2EtOH	5 ·4CHCl ₃
Pd–Cl	2.297(1)	2.3059(8)	2.3074(5)	2.2924(8)
Pd–P	2.3398(8)	2.3445(8)	2.3568(5)	2.3320(7)
Cl–Pd–P ^b	94.84(3)	88.10(3)	95.48(2)	90.33(3)
Fe–Cg1	1.650(2)	1.650(2)	1.6478(8)	1.647(1)
Fe–Cg2	1.645(2)	1.647(2)	1.6396(9)	1.650(1)
<Cp1,Cp2	2.7(2)	4.4(2)	4.9(1)	1.8(2)
τ^c	139	142	140	142
C11–O1	1.238(4)	1.235(4)	1.237(2)	1.241(4)
C11–N	1.339(5)	1.330(5)	1.349(2)	1.349(4)
O1–C11–N	121.5(3)	121.6(3)	119.8(2)	120.0(3)
ϕ^d	22.9(4)	12.9(4)	21.4(2)	20.2(4)
N–C24–C25–O2	–63.7(4)	60.4(4)	53.3(2) ^e	60.8(4) ^f

^a Definition of the ring planes: Cp1 = C(1–5), Cp2 = C(6–10); Cg1 (Cg2) are the centroids of the cyclopentadienyl rings Cp1 (Cp2). The primed atoms are generated by the crystallographic inversion operations.

^b The sum of the Cl–Pd–P and Cl–Pd–P' is 180° due to the imposed symmetry.

^c Torsion angle C1–Cg1–Cg2–C6.

^d Dihedral angle subtended by the Cp1 and {C11O1N} planes.

^e N–C26–C27–O3 = 47.1(2)°.

^f N–C26–C27–O3 = 178.5(3)°.

The individual geometric parameters as well as the overall molecular conformation compare favourably with those reported for complexes with other 1'-functionalised (diphenylphosphanyl)ferrocenes, *trans*-[PdCl₂(Ph₂PfcX-κP)₂] (fc = ferrocene-1,1'-yl; X = CO₂H [16], C(O)NHCH₂CH₂(C₅H₄N-2) [11a], PO₃Et₂ [17], CH=CH₂ [18], a chiral oxazolonyl group [9], P(O)Ph₂, [19] and SMe [20]). The bond distances and angles in the coordinated ferrocene ligands

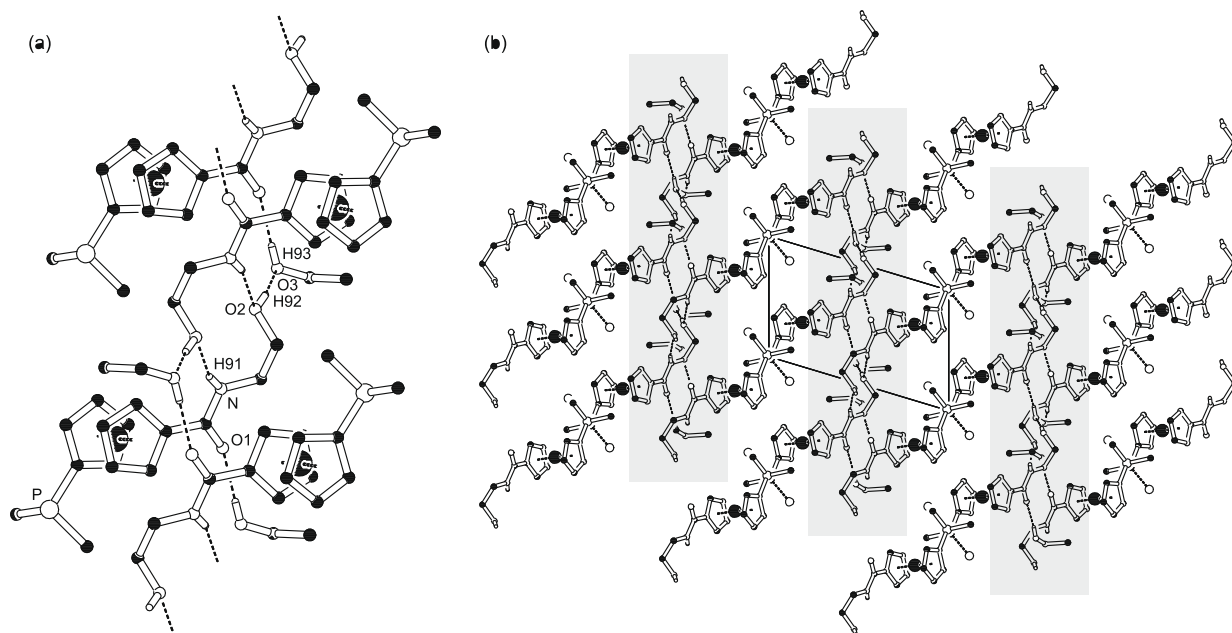


Fig. 8. (a) Section of the infinite hydrogen bonded array in the structure of **4·2EtOH**. (b) Projection of the crystal assembly onto the crystallographic *ac* plane. Domains accommodating the hydrogen-bonded layers are indicated with gray boxes. The hydrogen bonds are indicated with dashed lines (only hydrogen bonded H-atoms are shown). For clarity, the PdCl₂ moieties are omitted in part (a), and only pivotal carbon atoms from the phenyl rings and one position of the disordered CH₂ group in the solvent molecule are shown (parts a and b).

do not depart much from those in free ones. Some differences can be found in the conformation of the ferrocene framework. The ferrocene substituents in **4** and **5** are mutually rotated to attain more distant positions (*cf.* τ in Table 2) such that avoid their spatial contacts and facilitate hydrogen bond formation.

As with the free ligands, the crystal packing of the complexes is dominated by hydrogen bonds between the amide moieties. Complexity of the formed assemblies roughly parallels that of the respective ligands but it is further increased owing to the presence of *two* ligands per the complex molecule and the presence of the solvents of crystallisation. In the crystals of **4·2EtOH**, the hydrogen bonding interactions (Fig. 8) give rise to polar layers oriented perpendicular to the crystallographic *ac* plane. Since the two *trans*-disposed ligand moieties are the parts of different layers, the PdCl₂ unit interconnects two adjacent polar domains that are separated by the non-polar phosphano-ferrocenyl units. The basic hydrogen-bonded unit in the structure of **4·2EtOH** comprises two inversion-related ligand units from two different complex molecules that are linked by N–H···OH hydrogen bonds (Fig. 8a, Table 1). The remaining OH groups of the ligand form additional hydrogen bonds towards oxygen atoms in the solvent of crystallisation (O–H···O(EtOH)). The solvate molecules further interact with the proximal dimer units via (EtOH)O–H···O=C hydrogen bonds and thus interconnect the dimer units located above and below into the wall-like molecular architecture mentioned above.

In comparison with the ethanol solvate, the crystal packing of **4·6CHCl₃** is relatively simple. The amide pendants in **4·6CHCl₃** associate in only one dimension, forming infinite chains (Fig. 9). However, since these chains involve molecules from two complex molecules related by the 2₁ screw axes, the intermolecular interactions result in the formation of layers in the *ac* plane. Similarly to the ethanol solvate, the phosphano-ferrocenyl units in **4·6CHCl₃** are located between the hydrogen-bonded sheets, leaving enough space for the solvent molecules that occupy cylindrical voids oriented parallel to the crystallographic *b* axis.

Likewise free **2**, the solvate **5·2EtOH** aggregates into infinite chains in the crystal (Fig. 10). Nonetheless, the modes of aggrega-

tion noticeably differ in both compounds. Because of the imposed symmetry, the polar groups capable of hydrogen bonding in **5·2EtOH** are *anti*-arranged and, hence, appropriately set up for linear propagation of the molecular array. The key feature of the crystal packing of **5·2EtOH** is a centrosymmetric cyclic assembly

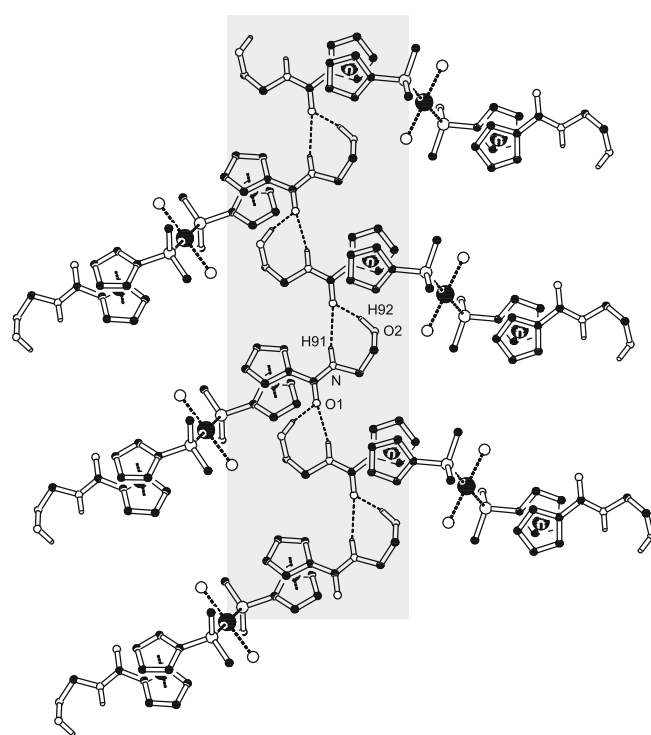


Fig. 9. Hydrogen bonding interactions in **4·6CHCl₃**. For clarity, only the pivotal phenyl carbons and hydrogen-bonded H-atoms are shown and the solvent molecules are omitted.

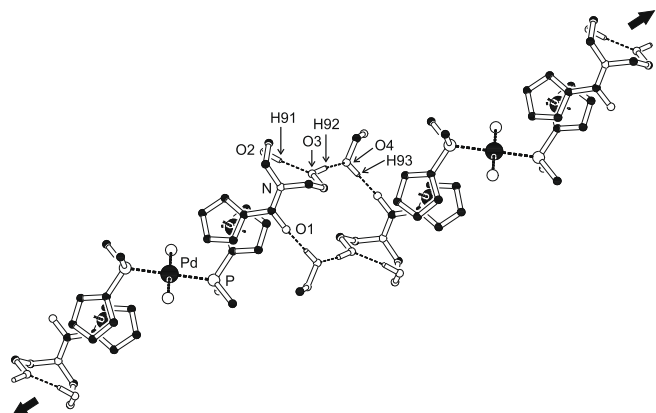


Fig. 10. Hydrogen bonding interactions in solid **5**·2EtOH. Only the pivotal phenyl carbons and H-bonded hydrogen atoms are shown for clarity.

(Fig. 10, Table 1) formed via four O–H···O hydrogen bonds between two ligand moieties (located in two proximal complex molecules) and two molecules of the solvent. The ethanol solvate acts as a molecular ‘clamp’, serving both as a hydrogen bond donor for the C=O group in one ligand and as an acceptor for the OH group in the other. The other terminal OH group of the ligand does not participate in intermolecular aggregation, being involved in an intramolecular O–H···O interaction.

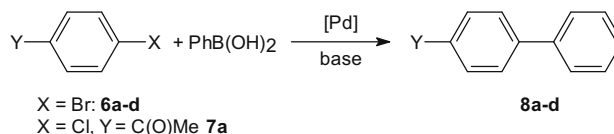
The crystal assembly of **5**·4CHCl₃ (Fig. 11) differs from that of the corresponding ethanol solvate in that each ligand moiety forms a cyclic dimer with its inversion-related counterpart through pairs of O3–H92···O1 hydrogen bonds (Table 1). These dimers further aggregate into infinite ladder-like array by means of O2–H91···O3 hydrogen bonds generated by the second hydroxyethyl chain (translation in the *a*-direction). Since each complex molecule possesses two ligand units, the ladder arrays are cross-linked by the PdCl₂ units into infinite layers. In contrast to the ethanol solvate, the solvent molecules in **5**·4CHCl₃ are only spectators in the crystal assembly, filling vacancies between the bulky complex molecules. Only one of the two structurally independent CHCl₃ mole-

cules forms hydrogen bonds to the Pd-bound chloride ligand (Table 1).

2.3. Catalytic tests

For catalytic testing of the complexes **4** and **5**, we chose Suzuki–Miyaura cross-coupling [21], which is an obvious candidate among the cross-coupling reactions for performing it in polar and aqueous solvents because of hydrolytic stability of boron reagents [4,22]. Initially, we probed complexes **4** and **5** as defined pre-catalysts in the model coupling of phenylboronic acid and 4-bromoacetophenone (**6a**) to give biphenyl **8a** (Scheme 4). The reactions were carried out in various solvents in the presence of potassium carbonate as the base and catalyst amount corresponding to 1 mol.% Pd at 60 °C for 24 h. The results given in Table 3 indicate that both complexes efficiently promote the coupling reaction, compound **4** showing slightly better conversions. The higher catalytic activity of complex **4** (or catalyst formed thereof) presumably reflects a higher stability of this complex under the reaction conditions which, in turn, parallels the higher hydrolytic stability of ligand **1**. When ligands **1** and **2** were heated with 5 mole equivalents of K₂CO₃ in ethanol (80 °C/2 h) to mimic the conditions of the catalysed reaction, the former compound was isolated virtually unchanged (contaminated with <2 mol% of the corresponding phosphane oxide) whilst for the tertiary amide, a mixture of unchanged **2** (73%), its P-oxide (ca. 1%) and two unidentified hydrolytic products (11 and 15%; not the parent Hdpf or its P-oxide) was obtained. Finally, the reactions performed in dioxane and acetonitrile gave lower yields than those carried out in ethanol, water and, surprisingly, even in the respective aqueous solvents.

Since the kinetic tests revealed that the model reaction proceeds rapidly, affording quantitative isolated yields of **8a** within 1 h in both water and ethanol under mild conditions (60 °C), we extended our study towards reactions in water–toluene biphasic mixture and also lowered the catalyst loading to 0.1 mol%. The more stable pre-catalyst **4** was tested in the coupling of PhB(OH)₂ with aryl bromides possessing activating and deactivating groups (**6a–d**, Scheme 4). The coupling reactions performed in biphasic mixture (Table 4) proceed satisfactorily only with the activated substrates **6a** and **6b**. Nevertheless, the results achieved with **4**



Scheme 4. Suzuki–Miyaura reaction of aryl bromides with PhB(OH)₂ [Y = C(O)Me (a), NO₂ (b), Me (c), OMe (d)].

Table 3
Survey of the reaction Solvents for the model coupling reaction.^a

Solvent	Conversion to 8a (%) ^b	
	Catalyst 4	Catalyst 5
Dioxane	85	94
Dioxane–water (1/1)	Quant. (96)	Quant. (96)
Ethanol	Quant. (99)	Quant. (97)
Ethanol–water (1/1)	Quant. (98)	Quant. (97)
MeCN	84	75
MeCN–water (1/1)	Quant. (99)	Quant. (94)
Water	Quant. (95)	Quant. (94)

^a Reaction of **6a** (1 mmol), PhB(OH)₂ (1.2 mmol), and K₂CO₃ (2 mmol) with 1 mol% Pd-catalyst in 5 ml of the solvent at 60 °C for 24 h.

^b The cases where no aryl halide was detectable by NMR, the conversions were considered to be quantitative (quant.; ≥99%). Isolated yields in parentheses. All values are an average of two independent runs.

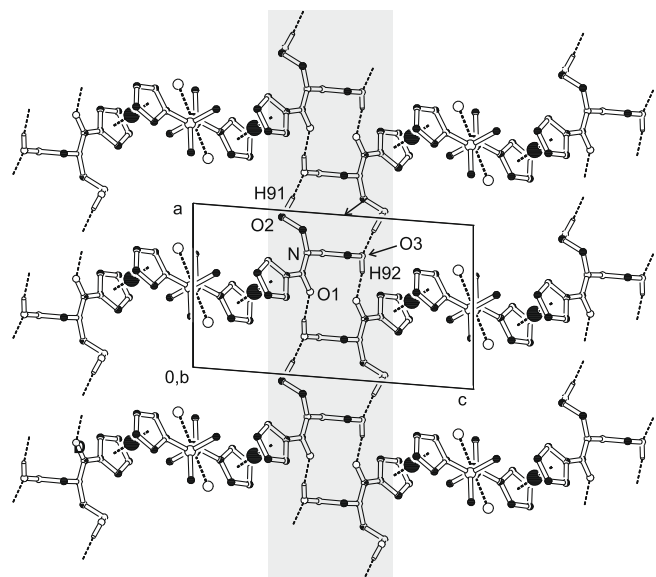


Fig. 11. View of the hydrogen-bonded layer in the structure of **5**·4CHCl₃ as projected onto the crystallographic *ac*-plane. For clarity, only pivotal phenyl carbons and hydrogen-bonded H-atoms are shown and the solvent molecules are omitted.

Table 4

Summary of the catalytic results for the reactions performed in toluene–water biphasic mixture.^a

Substrate	Product	Conversion with catalyst 4 (%)	
		1 mol%	0.1 mol%
4-YC ₆ H ₄ Br			
Y = C(O)Me	8a	Quant.	86
NO ₂	8b	64	47
Me	8c	28	27
OMe	8d	18	16

^a Conditions: water–toluene (1/1), 1 mol% of **4**, 1.2 equiv. PhB(OH)₂, 2 equiv. K₂CO₃, 60 °C/1 h.

were better than those attained with the related complex [PdCl₂(Hdpf-κP)₂] [16], which gave **8a** with 85% conversion under otherwise identical conditions. Replacing **6a** for the less reactive [4,22,23] 4-chloroacetophenone (**7a**) ensued in a considerably lower yield of the coupling product **8a** (conversions with 1 mol% of **4**: ca. 4% after 1 h, and 11% after 24 h at 60 °C).

Any direct comparison of **4**- and **5**-based catalysts with other systems is rather difficult due to varying reaction conditions (substrate, solvent, temperature, and catalyst loading). Notwithstanding, the conversions achieved with **4**- and **5**-based catalysts in *homogenous* reaction media compare favourably to those reported for catalysts based on sulphonated [24], R₃N⁺-substituted [25] or dendrimeric [26] phosphanes while being inferior to catalysts based on (biphenyl-2-yl)phosphanes [27]. Similar applies also to pure water and water–toluene biphasic system [25b,28] except that our catalysts do *not* require the presence of phase-transfer reagents for the coupling reaction to proceed efficiently.

Since the reactions performed under biphasic conditions are particularly attractive due to simple reaction setup, easy product separation and facile recovery of the catalyst ‘phase’ [4,22,28], we studied next the possibility of catalyst recycling. The reactions were performed in toluene–water mixture with complexes **4** and **5** at 1 mol% Pd loading. After heating to 60 °C for 1 h organic layers were separated and replaced with those containing fresh reagents. The results are presented graphically in Figs. 12 and 13. At first sight, the results reflect the higher stability of the catalytic system based on **4** (*vide supra*), which retained its original high activity unchanged (complete conversions, isolated yields ≥94%) during five consecutive runs. By contrast, the catalyst resulting from **5** showed a lower initial conversion and a steady decline in the activity with a sharp drop after the fourth run.

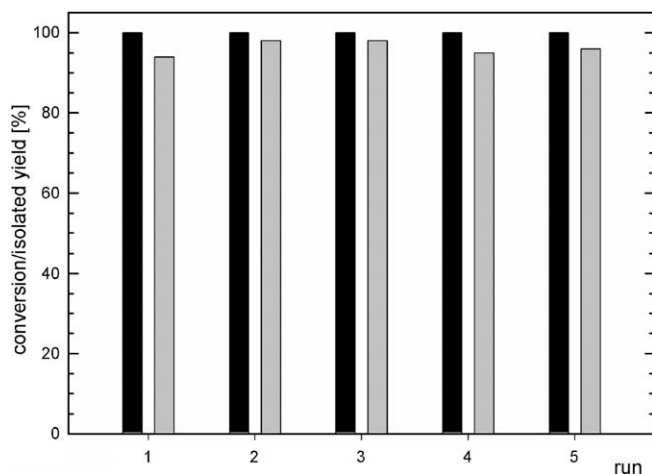


Fig. 12. Recycling tests with pre-catalyst **4** (conversions in black, isolated yields in grey).

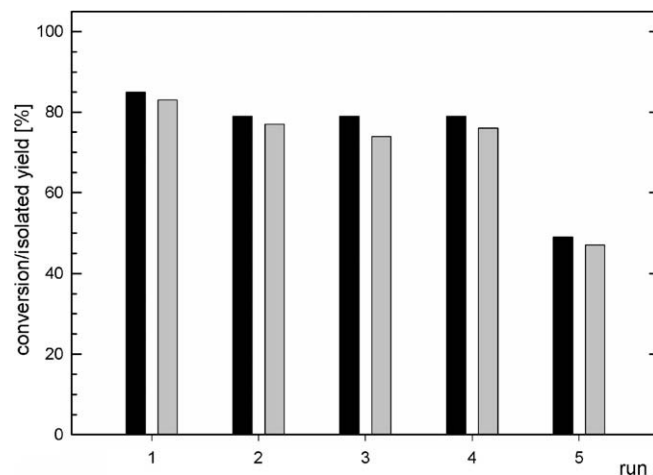
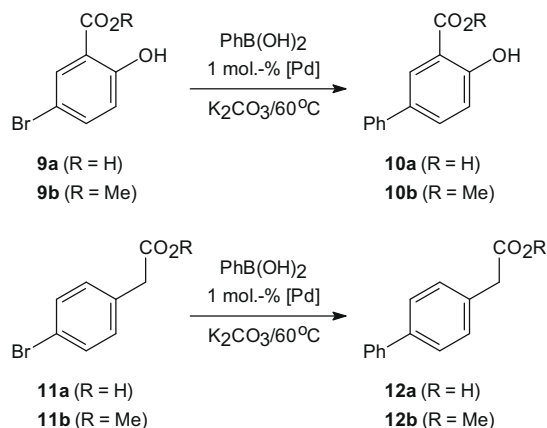


Fig. 13. Recycling tests with pre-catalyst **5** (conversions in black, isolated yields in grey).



Scheme 5.

These results encouraged us to study biaryl couplings with substrates that can either react with bases (esters) or possess dissociable polar groups (carboxylic acids). For testing we chose the preparation of non-steroidal anti-inflammatory drugs and their model compounds: 5-phenylsalicylic acid (**10a**) as a model for 5-(2,4-difluorophen-yl)-2-hydroxybenzoic acid (DiflunisalTM), and (biphenyl-4-yl)acetic acid (**12a**; FelbinacTM) [22c,29,30]. The syntheses were carried out with free acids (**10a**, **12a**) and their respec-

Table 5

Application of complex **4** to the synthesis of **10a,b** and **12a,b**.^a

Substrate	Solvent	Time (h)	Product	Yield (%) ^b
9a	W	1	10a	53
9a	W	24	10a	83
9a	B	24	10a	84
11a	W	1	12a	63
11a	W	24	12a	94
11a	B	24	12a	Quant.
9b	B	1	10b	86
9b	B	24	10b	Quant.
11b	B	1	12b	74
11b	B	24	12b	Quant.

^a Conditions: 1 mol% of **4**, 1.2 equiv. PhB(OH)₂, 2 equiv. K₂CO₃, 60 °C. B, biphasic mixture toluene–water (1/1), W, water. See Section 3 for details.

^b Isolated yields.

tive methyl esters (**10b**, **12b**; Scheme 5) in the biphasic system and in the presence of complex **4** (1 mol% Pd).

The results (Table 5) confirm that even free acids can be efficiently coupled in water and in toluene–water biphasic mixture with catalyst **4**, affording the respective carboxyl-substituted biphenyls in excellent isolated yields. Esters **9b** and **11b** also reacted smoothly in the toluene–water mixture to give good yields of the respective coupling products even after 1 h.

3. Conclusions

Introduction of amide moieties equipped with hydrophilic substituents offers an alternative approach towards the design of novel phosphinoferrrocene ligands suitable for polar reaction media including water-containing ones. Even the relatively simple hydroxyethyl-substituted amide moieties present in the molecules of **1** and **2** improve water-solubility of such donors and their complexes. Complexes **4** and **5** can thus serve as defined pre-catalysts for Suzuki–Miyaura cross-coupling of aryl bromides with boronic acids in polar organic solvents, water and in toluene–water biphasic mixtures. Yet, compound **4** appears to be practically more useful, affording a faster reacting and more robust (hydrolytically stable) catalyst, which can be conveniently re-used in toluene–water mixture. Ligand **1** thus constitutes an alternative to the commonly used non-polar ferrocene ligands [1,2,31]. Furthermore, amido-phosphanes **1** and **2** hold considerable potential for the design of self-assembled organometallic supramolecular arrays [32]. This was demonstrated by the crystal structures of free ligands and their solvated complexes, which are dominated by hydrogen bonding interactions of the amide groups and polar solvent molecules (where present), and distinctively change along with the structure of the ligand (its amide pendant) and the type and amount of the solvent molecules.

4. Experimental

4.1. Materials and methods

The syntheses were performed under an argon atmosphere. Dichloromethane was dried over anhydrous K_2CO_3 or CaH_2 and distilled. Dioxane and acetonitrile were dried over sodium metal and K_2CO_3 , respectively, and distilled. 2-Aminoethanol was distilled under reduced pressure. Hdpf [8a], $[PdCl_2(cod)]$ [33], and **9b** [34] were prepared by the literature methods. Ester **11b** [35] was obtained by esterification of **11a** with diazomethane. Other chemicals and solvents were used without any purification.

NMR spectra were measured on a Varian Unity Inova 400 spectrometer (1H , 399.95; ^{13}C , 100.58; ^{31}P , 161.90; ^{19}F , 376.29 MHz) at 25 °C unless indicated otherwise. Chemical shifts (δ /ppm) are given relative to internal $SiMe_4$ (^{13}C and 1H), external 85% aqueous H_3PO_4 (^{31}P) or neat $CFCl_3$ (^{19}F). IR spectra were recorded with an FTIR Nicolet Magna 650 spectrometer. Positive-ion electron impact (EI+) mass spectra including the high resolution (HR) data were obtained with a ZAB EQ spectrometer (VG Analytical). Electrospray (ESI±) mass spectra were recorded with a Bruker Esquire 3000 spectrometer on dichloromethane/methanol solutions. Melting points were determined on a Kofler hot stage.

4.2. Preparation of 1-(diphenylphosphanyl)-1'-[N-(2-hydroxyethyl)-carbamoyl]ferrocene (**1**)

Hdpf (1.244 g, 3.0 mmol) and 1-hydroxybenzotriazole (0.476 g, 3.5 mmol) were dissolved in dichloromethane (45 mL). The solution was cooled in an ice bath and treated with *N*-ethyl-*N'*-[3-(dimethylamino)propyl]carbodiimide (0.62 mL, 3.5 mmol). After stirring for 30 min at 0 °C, neat 2-aminoethanol (0.23 mL,

3.8 mmol) was added, causing an immediate (partial) precipitation. The cooling bath was removed and stirring was continued at room temperature for 16 h. Then, the reaction mixture was washed with 3 M HCl, the organic layer was separated, and the aqueous phase was back-extracted with dichloromethane (2 × 10 mL). The combined organic layers were washed with saturated aqueous $NaHCO_3$ and brine, dried over $MgSO_4$, and evaporated under vacuum. The orange residue was purified by column chromatography (silica gel, CH_2Cl_2 –methanol 10:1 v/v). The first, minor band was discarded and the following, major orange band was collected and evaporated to afford an orange glassy residue. This crude product was immediately dissolved in hot ethyl acetate (30 mL), the solution was mixed with hexane (30 mL) and allowed to crystallise at room temperature and then at 4 °C. The separated solid was filtered off, washed with hexane and dried under vacuum. Yield: 1.120 g (82%), orange crystalline solid.

M.p. 135–137 °C. 1H NMR ($CDCl_3$): δ 3.39 (br s, 1H, OH), 3.49 (br dt, $J_{HH,1} \approx J_{HH,2} \approx 4.3$ Hz, 2H, NCH_2), 3.75 (br t, $^3J_{HH} = 4.6$ Hz, 2H, OCH_2), 4.09 (apparent q, $J' = 1.9$ Hz, 2H), 4.22 (apparent t, $J' = 1.9$ Hz, 2H), 4.44 (apparent t, $J' = 1.8$ Hz, 2H), 4.60 (apparent t, $J' = 2.0$ Hz, 2H) (CH of fc); 6.34 (br t, $^3J_{HH} \approx 5.6$ Hz, 1H, NH), 7.27–7.41 (m, 10H, PPh_2). $^{13}C\{^1H\}$ NMR ($CDCl_3$): δ 42.7 (NCH_2), 62.6 (OCH_2), 69.6 (d, $J_{PC} \approx 1$ Hz), 71.6, 72.8 (d, $J_{PC} = 4$ Hz), 74.5 (d, $J_{PC} = 14$ Hz) (CH of fc); 76.3 (C–CO of fc), 77.1 (d, $^1J_{PC} = 6$ Hz, C–P of fc), 128.3 (d, $J_{PC} = 7$ Hz), 128.8, 133.4 (d, $J_{PC} = 19$ Hz) (CH of PPh_2); 138.1 (d, $^1J_{PC} = 8$ Hz, C_{ipso} of PPh_2), 171.3 (C=O). $^{31}P\{^1H\}$ NMR ($CDCl_3$): δ –17.1 (s). IR (Nujol): ν/cm^{-1} 3293 (br s), 1633 (s), 1583 (w), 1552 (s), 1295 (s), 1193 (s), 1159 (s), 1055 (m), 1027 (s), 1008 (m), 916 (m), 889 (m), 833 (m), 822 (m), 749 (s), 741 (s), 696 (s), 636 (m), 569 (m), 550 (m), 516 (s), 505 (s), 489 (s), 453 (s), 421 (m). Anal. Calc. for $C_{25}H_{24}FeNO_2P$ (457.3): C, 65.66; H, 5.29; N, 3.06. Found: C, 65.39; H, 5.14; N, 2.83%.

4.3. Preparation of pentafluorophenyl 1-(diphenylphosphanyl)ferrocene-1-carboxylate (**3**)

Hdpf (2.075 g, 5.0 mmol), pentafluorophenol (1.104 g, 6.0 mmol), *N*-ethyl-*N'*-[3-(dimethylamino)propyl]carbodiimide hydrochloride (1.160 g, 6.0 mmol) and 4-(dimethylamino)pyridine (0.122 g, 1.0 mmol) were dissolved in CH_2Cl_2 (50 mL) and the resulting solution was stirred at room temperature for 20 h. The reaction mixture was washed with brine (2 × 20 mL), dried over $MgSO_4$ and evaporated. The residue was purified by column chromatography (silica gel, hexane–diethyl ether 1:1 v/v) to yield, after evaporation, pure ester **3** as an orange solid. Yield: 2.419 g (83%).

1H NMR ($CDCl_3$): δ 4.25 (apparent q, $J' = 1.9$ Hz, 2H), 4.44 (apparent t, $J' = 2.0$ Hz, 2H), 4.55 (apparent t, $J' = 1.8$ Hz, 2H), 4.87 (apparent t, $J' = 2.0$ Hz, 2H) (fc); 7.29–7.39 (m, 10H, PPh_2). $^{13}C\{^1H\}$ NMR ($CDCl_3$): δ 67.6 (C–CO), 71.8, 73.6 (d, $J_{PC} = 4$ Hz), 74.3 (d, $J_{PC} = 2$ Hz), 74.7 (d, $J_{PC} = 14$ Hz) (CH of fc); 79.1 (d, $J_{PC} = 10$ Hz, C–P of fc), 128.3 (d, $^3J_{PC} = 7$ Hz), 128.8, 133.4 (d, $^2J_{PC} = 20$ Hz) (CH of PPh_2); 137.9 (dm, $^1J_{FC} = 255$ Hz, C_{meta} of C_6F_5), 138.2 (d, $J_{PC} = 10$ Hz, C_{ipso} of PPh_2), 139.3 (dm, $^1J_{FC} = 253$ Hz, C_{para} of C_6F_5), 141.3 (dm, $^1J_{FC} = 250$ Hz, C_{ortho} of C_6F_5); 167.6 (C=O). The resonance due to $C_{ipso}(C_6F_5)$ was not found. $^{19}F\{^1H\}$ NMR ($CDCl_3$): δ –162.8 (m, F_{meta}), –158.7 (t, $^3J_{FF} = 22$ Hz, F_{para}), –152.9 (m, F_{ortho}) (C_6F_5). $^{31}P\{^1H\}$ NMR ($CDCl_3$): δ –17.8 (s). MS (EI+): m/z (relative abundance) 580 (M^+), 488 (11), 413 (4, $[M-C_6F_5]^+$), 397 (26, $[M-OC_6F_5]^+$), 370 (19), 305 (35), 183 (18), 171 (19), 149 (40). HR MS (EI+) calcd. for $C_{29}H_{18}O_2F_5P^{56}Fe$ 580.0314, found 580.0297.

4.4. Preparation of 1-(diphenylphosphanyl)-1-[*N,N*-bis(2-hydroxyethyl)-carbamoyl]ferrocene (**2**)

Ester **3** (1.161 g, 2.0 mmol), diethanolamine (0.421 g, 4 mmol) and 4-(dimethylamino)pyridine (61 mg, 0.5 mmol) were dissolved

in dry DMF (15 mL) under argon. The reaction mixture was stirred at room temperature for 20 h, evaporated under vacuum, and the residue was purified by column chromatography (silica gel, dichloromethane–methanol 10:1 v/v). The first orange band was collected and evaporated to give **2** as orange-brown viscous oil that slowly solidified. The product was further crystallised by dissolving in a hot mixture of ethyl acetate and hexane (1:2 v/v) and slow cooling to -18°C . The separated material was filtered off, washed with hexane and diethyl ether, and dried under vacuum. Yield of **2**: 0.695 g (70%), orange crystalline solid.

M.p. 128–130 $^{\circ}\text{C}$. ^1H NMR (CDCl_3): δ 3.40 (br s, 2H, OH), 3.69 and 3.87 (2 \times br s, 4H, $\text{NCH}_2\text{CH}_2\text{OH}$); 4.11 (apparent q, $J' = 1.9$ Hz, 2H), 4.20 (apparent t, $J' = 2.0$ Hz, 2H), 4.47 (apparent t, $J' = 1.8$ Hz, 2H), 4.68 (apparent t, $J' = 2.0$ Hz, 2H) (CH of fc); 7.29–7.38 (m, 10 H, PPh_2). $^{13}\text{C}\{^1\text{H}\}$ NMR (CDCl_3): 50.7, 52.9 (2 \times br s, NCH_2); 61.2 (br, OCH_2), 71.2, 72.0, 73.2, 74.5 (br d, $J_{\text{PC}} = 14$ Hz) (CH of fc); 78.4 (C–CO of fc), 128.3 (br d), 128.7, 133.5 (br d, $J_{\text{PC}} = 20$ Hz) (CH of PPh_2); 138.4 (br, C_{ipso} of PPh_2), 172.6 (br) (C=O). The signal of C(fc)–P was not observed, probably due to overlaps. $^{31}\text{P}\{^1\text{H}\}$ NMR (CDCl_3): δ -17.1 (s). IR (Nujol): ν/cm^{-1} 3449 (s), 3282 (s), 1594 (s), 1366 (w), 1350 (w), 1330 (w), 1271 (m), 1192 (m), 1162 (m), 1093 (m), 1070 (s), 1043 (m), 919 (w), 885 (m), 836 (w), 821 (w), 747 (s), 697 (s), 676 (m), 522 (m), 495 (s), 447 (m), 422 (m). Anal. Calc. for $\text{C}_{27}\text{H}_{28}\text{FeNO}_3\text{P}$ (501.3): C 64.68, H 5.63, N 2.79. Found: C 63.58, H 5.65, N 2.67%.

4.5. Preparation of complex $[\text{PdCl}_2(\text{1-P})_2]$ (**4**)

$[\text{PdCl}_2(\text{cod})]$ (28.5 mg, 0.1 mmol) and **1** (91.4 mg, 0.2 mmol) were dissolved in dichloromethane (5 mL) and the resulting red solution was stirred for 30 min. The solution was filtered (PTFE syringe filter, 0.45 μm pore size) and the filtrate evaporated under vacuum. The crude product was crystallised from hot ethanol (10 mL). The separated crystalline product was isolated by suction, washed with diethyl ether and dried under vacuum. Yield of **4**·2EtOH: 103 mg (91%), red crystalline solid. Solvate **4**·6 CHCl_3 resulted by crystallisation from CHCl_3 .

^1H NMR (CDCl_3 , 50 $^{\circ}\text{C}$): δ 2.83 (t, $J_{\text{HH}} = 4.6$ Hz, 1H, OH), 3.38 (q, $J_{\text{HH}} = 5.2$ Hz, 2H) and 3.68 (q, $J_{\text{HH}} = 5.0$, 2H) (CH_2CH_2); 4.51 (apparent t, $J' = 1.9$ Hz, 2H), 4.56 (apparent t, $J' = 2.0$ Hz, 2H), 4.57 (br apparent t, $J' \approx 1.9$ Hz, 2H), 4.90 (apparent t, $J' = 2.0$ Hz, 2H) (fc); 6.45 (t, $J_{\text{HH}} = 5.5$ Hz, 1H, NH), 7.36–7.68 (m, 10H, PPh_2). $^{31}\text{P}\{^1\text{H}\}$ NMR (CDCl_3 , 50 $^{\circ}\text{C}$): δ +16.2 (s). IR (Nujol): ν/cm^{-1} 3242 (bs), 2725 (w), 2360 (m), 1629 (m), 1541 (m), 1541 (m), 1297 (m), 1165 (m), 1073 (m), 694 (m), 536 (m), 504 (m). Anal. Calc. for $\text{C}_{50}\text{H}_{60}\text{Fe}_2\text{N}_2\text{O}_6\text{P}_2\text{Cl}_2\text{Pd}$ (**4**·2EtOH; 1135.94): C, 52.86; H, 5.32; N, 2.47. Found: C, 52.98; H, 4.97; N 2.20%.

4.6. Preparation of complex $[\text{PdCl}_2(\text{2-P})_2]$ (**5**)

$[\text{PdCl}_2(\text{cod})]$ (28.5 mg, 0.1 mmol) and ligand **2** (100 mg, 0.2 mmol) were dissolved in dichloromethane (5 mL). The resulting solution was stirred for 30 min whereupon the product separated. The precipitate was filtered off, washed with diethyl ether and pentane, and dried under vacuum. Another crop was obtained by precipitation of the mother liquor with pentane. Combined yield of **5**: 90 mg (76%), orange solid. The precipitated product tends to hold solvents; defined solvates resulted upon crystallisation from EtOH or CHCl_3 .

^1H NMR (CDCl_3): δ 3.64 and 3.83 (2 \times br s, 4H, CH_2CH_2); 4.55 (br m, 2H), 4.58 (apparent t, $J' = 1.8$ Hz, 2H), 4.66 (br m, 2H), 4.84 (apparent t, $J' = 1.9$ Hz, 2H) (fc); 7.36–7.65 (m, 10H, PPh_2). $^{31}\text{P}\{^1\text{H}\}$ NMR (CDCl_3): δ +16.6 (s). IR (Nujol): ν/cm^{-1} 3299 (s), 1588 (vs), 1304 (m), 1271 (w), 1164 (m), 1048 (m), 938 (w), 898 (w), 841 (w), 746 (w), 692 (m), 627 (w), 514 (w), 500 (m), 473

(w). Anal. Calc. for $\text{C}_{54}\text{H}_{56}\text{Fe}_2\text{N}_2\text{O}_6\text{P}_2\text{Cl}_2\text{Pd}\cdot\text{CH}_2\text{Cl}_2$ (1264.02): C, 52.22; H, 4.62; N, 2.22. Found: C, 51.84; H, 4.47; N, 2.15%.

4.7. Catalytic tests

Reaction vessel (20 mL) was charged with phenylboronic acid (146 mg, 1.2 mmol), K_2CO_3 (276.5 mg, 2.0 mmol), aryl halide (1.0 mmol) and the catalyst (1 or 0.1 mol% of **4** or **5**). After flushing with argon, solvent (5 mL) was introduced and the reaction flask was sealed and transferred to an oil bath maintained at 60 $^{\circ}\text{C}$. The reaction mixture was heated and stirred for 1 or 24 h and then quenched by adding water (5 mL) and stirring for 15 min. The resulting mixture was extracted with diethyl ether (3 \times 5 mL), the organic layers were combined, dried over MgSO_4 , and evaporated. Subsequent purification by column chromatography (silica gel and diethyl ether) afforded the coupling products (in the case of incomplete conversion contaminated with the starting halide). The identity and purity (conversion) of the products was established by ^1H NMR spectra.

4.8. Catalyst recycling tests

The initial reaction mixture was prepared as described above by mixing $\text{PhB}(\text{OH})_2$ (146 mg, 1.2 mmol), K_2CO_3 (276.5 mg, 2.0 mmol), 4-bromoacetophenone (199 mg, 1.0 mmol), the catalyst (1 mol% of **4** or **5**), and toluene and water (3 mL each). The mixture was heated to 60 $^{\circ}\text{C}$ while stirring for 1 h and then cooled in ice. The cold reaction mixture was washed with hexane (2 \times 5 mL) and the organic layers were decanted to collect the coupling product. The organic solutions were washed with saturated aqueous K_2CO_3 (2 \times 5 mL), dried (MgSO_4), and the product was isolated as described above.

To the aqueous layer were immediately added $\text{PhB}(\text{OH})_2$ (122 mg, 1.0 mmol), 4-bromoacetophenone (199 mg, 1.0 mmol), K_2CO_3 (138 mg, 1.0 mmol) and toluene (3 mL). The resulting biphasic mixture was used in the next catalytic run (60 $^{\circ}\text{C}/1$ h) and treated as described above. For each pre-catalyst, such recycling was repeated four times.

4.9. Catalytic synthesis of **10a** and **12a**

A Schlenk tube was charged with $\text{PhB}(\text{OH})_2$ (146 mg, 1.2 mmol), K_2CO_3 (276 mg, 2.0 mmol), aryl bromide (**9a** or **11a**, 1.0 mmol), and the catalyst (1 mol% of **4**). Water (5 mL) or water and toluene (3 mL each) were added, and the reaction flask was flushed with argon, sealed with septum and transferred to an oil bath kept at 60 $^{\circ}\text{C}$. After stirring for the reaction time (1 or 24 h), the mixture was cooled, quenched by adding 3 M HCl (10 mL) and extracted with diethyl ether (4 \times 5 mL). Combined organic layers were washed with brine, dried (MgSO_4) and purified by flash chromatography (silica gel and diethyl ether). The products were isolated as white solids following solvent removal.

Analytical data for **10a**. ^1H NMR (DMSO): δ 7.07 (d, $J_{\text{HH}} = 8.5$ Hz, 1H), 7.32–7.63 (m, 6 H), 7.83 (dd, $J_{\text{HH}} = 8.7$, 2.6 Hz, 1H), 8.04 (d, $J_{\text{HH}} = 2.5$ Hz, 1H) (aromatics). $^{13}\text{C}\{^1\text{H}\}$ NMR (DMSO): δ 113.3, 117.7, 126.1, 127.0, 127.9, 127.9, 131.2, 133.8, 139.0, 160.5 (aromatics); 171.79 (C=O) [30c,i]. ESI-MS: m/z 213 ($[\text{M}-\text{H}]^-$).

Analytical data for **12a**. ^1H NMR (CDCl_3): δ 3.69 (s, 2H, CH_2), 7.13–7.61 (m, 9H, aromatics). $^{13}\text{C}\{^1\text{H}\}$ NMR (CDCl_3): δ 40.6 (CH_2); 127.1, 127.3, 127.4, 128.8, 129.8, 132.3, 140.4, 140.7 (aromatics); 177.2 (C=O) [30b,f,i,36]. ESI+MS: m/z 235 ($[\text{M}+\text{Na}]^+$).

4.10. Catalytic Preparation of **10b** and **12b**

Reaction flask was charged with $\text{PhB}(\text{OH})_2$ (146 mg, 1.2 mmol), K_2CO_3 (276 mg, 2.0 mmol), aryl bromide (**9b** or **11b**,

Table 6
Crystallographic data, data collection and structure refinement parameters for **1**, **2**, **4·2EtOH**, **4·6CHCl₃**, **5·2EtOH**, and **5·4CHCl₃**.^a

Compound	1	2	4·2EtOH	4·6CHCl₃	5·2EtOH	5·4CHCl₃
Formula	C ₂₅ H ₂₄ FeNO ₂ P	C ₂₇ H ₂₈ FeNO ₃ P	C ₅₄ H ₆₀ Cl ₂ Fe ₂ N ₂ O ₆ P ₂ Pd ^f	C ₅₆ H ₅₄ Cl ₂₀ Fe ₂ N ₂ O ₄ P ₂ Pd ^h	C ₅₈ H ₆₈ Cl ₂ Fe ₂ N ₂ O ₈ P ₂ Pd ^l	C ₅₈ H ₆₀ Cl ₁₄ Fe ₂ N ₂ O ₆ P ₂ Pd ^k
<i>M</i> (g mol ⁻¹)	425.27	501.32	1183.98	1808.05	1272.08	1657.42
Crystal system	Orthorhombic	Triclinic	Triclinic	Monoclinic	Triclinic	Triclinic
Space group	<i>Pccn</i> (No. 56)	<i>P</i> $\bar{1}$ (No. 2)	<i>P</i> $\bar{1}$ (No. 2)	<i>P</i> ₂ / <i>n</i> (no. 14)	<i>P</i> $\bar{1}$ (No. 2)	<i>P</i> $\bar{1}$ (No. 2)
<i>a</i> (Å)	14.3332(1)	8.3328(2)	8.8555(3)	18.2832(5)	10.1226(2)	9.5303(1)
<i>b</i> (Å)	36.4044(5)	8.9101(3)	11.6714(5)	10.3326(2)	12.4024(3)	11.0754(2)
<i>c</i> (Å)	8.0570(1)	16.9636(6)	13.4224(6)	19.0708(5)	12.4331(3)	16.1583(2)
α (°)		89.839(2)	98.978(2)		74.060(1)	90.7960(8)
β (°)		87.331(2)	103.252(3)	97.969(1)	72.918(1)	94.2906(9)
γ (°)		66.776(2)	106.257(3)		72.918(1)	99.4265(9)
<i>V</i> (Å ³)	4204.08(8)	1156.00(6)	1259.8(1)	3567.9(2)	1368.81(6)	1677.20(4)
<i>Z</i>	8	2	1	2	1	1
<i>D</i> _{calc} (g cm ⁻³)	1.445	1.440	1.561	1.683	1.543	1.641
μ (Mo K α) (mm ⁻¹)	0.816 ^e	0.752	1.144	1.489 ⁱ	1.061	1.340 ^l
Diffractions total	44 656	15 918	19 085	42 124	26 812	34 739
<i>R</i> _{int} (%) ^b	4.83	7.7	5.1	6.4	4.2	7.1
Unique diffns	4827	5195	5517	7801	6257	7750
Observed ^c diffns	4022	4638	4341	6417	5689	6691
<i>R</i> (obsd) (%) ^{d,c}	3.30	3.11	3.95	4.33	2.64	4.27
<i>R</i> , <i>wR</i> (all) (%) ^d	4.55, 7.73	3.65, 7.93	5.88, 9.34	5.74, 11.4	3.06, 6.57	5.14, 10.6
$\Delta\rho$ (e Å ⁻³)	0.30, -0.30	0.38, -0.42	0.94, -0.78 ^g	1.05, -1.30 ^g	0.46, -0.60	1.67, -1.19 ^g

^a Common details: *T* = 150(2) K.

^b $R_{int} = \sum |F_o^2 - F_o^2(\text{mean})| / \sum F_o^2$, where $F_o^2(\text{mean})$ is the average intensity for symmetry-equivalent diffractions.

^c Diffractions with $I_o > 2\sigma(I_o)$.

^d $R = \sum ||F_o| - |F_c|| / \sum |F_o|$, $wR = [\sum w(F_o^2 - F_c^2)^2 / \sum w(F_o^2)]^{1/2}$.

^e Corrected for absorption; the range of transmission coefficients = 0.778–0.945.

^f C₅₀H₄₈Cl₂Fe₂N₂O₄P₂Pd·2C₂H₆O.

^g Residual electron density in the space accommodating the solvent.

^h C₅₀H₄₈Cl₂Fe₂N₂O₄P₂Pd·6CHCl₃.

ⁱ Corrected for absorption; the range of transmission coefficients = 0.589–0.874.

^j C₅₄H₅₆Cl₂Fe₂N₂O₆P₂Pd·2C₂H₆O.

^k C₅₄H₅₆Cl₂Fe₂N₂O₆P₂Pd·4CHCl₃.

^l Corrected for absorption; the range of transmission coefficients = 0.505–0.910.

1.0 mmol), and the catalyst (1 mol% of **4**). Water and toluene were added (3 mL each), and the reaction flask was flushed with argon, sealed with septum and transferred to an oil bath maintained at 60 °C. After stirring for the reaction time (1 or 24 h), the mixture was cooled, diluted with water and extracted with diethyl ether. The organic extracts were washed with saturated aqueous K₂CO₃ solution, dried (MgSO₄) and passed through a short silica gel column, eluting with diethyl ether. Subsequent evaporation afforded the products as a white solid (**10b**) or a colourless oil (**12b**).

Analytical data for 10b. ¹H NMR (DMSO): δ 3.93 (s, 3H), 7.10 (d, 1H, $J_{\text{HH}} = 8.7$ Hz), 7.32–7.37 (m, 1H), 7.44–7.47 (m, 2H), 7.61–7.63 (m, 2H), 7.84 (m, 1H), 8.01 (d, 1H, $J_{\text{HH}} = 2.4$ Hz), 10.53 (br s, 1 H). ¹³C{¹H} NMR (DMSO): δ 52.4 (CH₃); 113.6, 118.0, 126.1, 127.1, 127.6, 128.9, 131.4, 133.7, 138.8, 159.2 (aromatics); 168.9 (C=O).^[37] ESI+ MS: *m/z* 251 ([M+Na]⁺); ESI- MS: *m/z* 227 ([M-H]⁻).

Analytical data for 12b. ¹H NMR (CDCl₃): δ 3.67 (s, 2H, CH₂), 3.71 (s, 3H, CH₃), 7.34–7.59 (m, 9H, aromatics). ¹³C{¹H} NMR (CDCl₃): δ 40.8 (CH₂), 52.1 (CH₃); 127.1, 127.3, 127.4, 129.7, 133.0, 140.1, 140.8 (aromatics); 172.1 (C=O) [30a,38]. ESI+ MS: *m/z* 249 ([M+Na]⁺).

4.11. X-ray crystallography

Single crystals suitable for diffraction analysis were grown by crystallisation from ethyl acetate–hexane (**1**: orange plate, 0.06 × 0.25 × 0.30 mm³; **2**: orange prism, 0.27 × 0.30 × 0.40 mm³), ethanol–diethyl ether (**4·2EtOH**: red plate, 0.05 × 0.10 × 0.30 mm³; **5·2EtOH**: red prism, 0.15 × 0.18 × 0.25 mm³),

and from chloroform (**4·6CHCl₃**: red plate, 0.10 × 0.35 × 0.55 mm³; **5·4CHCl₃**: red plate, 0.10 × 0.30 × 0.65 mm³).

The diffraction data ($\pm h\pm k\pm l$, $2\theta \leq 54$ – 55° , data completeness >97%) were collected with a Nonius KappaCCD diffractometer equipped with a Cryostream Cooler (Oxford Cryosystems) using graphite monochromatised Mo K α radiation ($\lambda = 0.71073$ Å) and were analysed with the HKL program package [39]. The structures were solved by direct methods (SIR97, Ref. [40]) and refined by full-matrix least-squares procedure based on F^2 (SHELXL97, ref. [41]). Non-hydrogen atoms were refined with anisotropic displacement parameters. Amide and hydroxyl hydrogens were identified on the difference electron density maps and refined as riding atoms. Other hydrogen atoms were included in their ideal positions and treated as riding atoms. The solvent molecule in **4·2EtOH** is disordered and was modelled over two positions (50:50) with the CH₃ and OH groups as the pivots.

Relevant crystallographic data are given in Table 6. Geometric parameters and structural drawings were obtained with a recent version of PLATON program [42]. All numerical values are rounded with respect to their estimated standard deviations (esd's) given with one decimal; parameters involving fixed hydrogen atoms are given without esd's.

5. Supplementary material

CCDC 711639, 711640, 711641, 711642, 711643 and 711644 contain the supplementary crystallographic data for this paper. These data can be obtained free of charge from The Cambridge Crystallographic Data Centre via www.ccdc.cam.ac.uk/data_request/cif.

Acknowledgements

This work is a part of the long-term research project of Faculty of Science, Charles University supported by the Ministry of Education, Youth and Sports of the Czech Republic (Nos. MSM0021620857 and LC 06070).

References

- [1] (a) P. Štěpnička (Ed.), *Ferrocenes: Ligands, Materials and Biomolecules, Part I – Ferrocene ligands*, Wiley, Chichester, 2008, pp. 3–277 (Chapters 1–7); (b) A. Togni, T. Hayashi (Eds.), *Ferrocenes: Homogeneous Catalysis Organic Synthesis Materials Science, Part I – Homogeneous Catalysis*, Wiley-VCH, Weinheim, 1995, pp. 3–142 (Chapters 1 and 2).
- [2] Recent reviews: (a) R.G. Arrayás, A. Adrio, J.C. Carretero, *Angew. Chem., Int. Ed.* 45 (2006) 7674; (b) R.C.J. Atkinson, V.C. Gibson, N.J. Long, *Chem. Soc. Rev.* 33 (2004) 313.
- [3] (a) B. Cornils, W.A. Herrmann (Eds.), *Aqueous-phase organometallic catalysis*, 2nd ed., Wiley-VCH, Weinheim, 2004; (b) F. Joó, *Aqueous Organometallic Catalysis*, Kluwer, New York, 2002.
- [4] (a) Recent review: N. Pinault, D.W. Bruce, *Coord. Chem. Rev.* 241 (2003) 1; (b) J.P. Genet, M. Savignac, *J. Organomet. Chem.* 576 (1999) 305.
- [5] B. Pugin, V. Groehn, R. Moser, H.-U. Blaser, *Tetrahedron: Asymmetry* 17 (2006) 544.
- [6] P. Štěpnička, *Eur. J. Inorg. Chem.* (2005) 3787.
- [7] Recent examples: (a) P. Štěpnička, I. Císařová, *Collect. Czech. Chem. Commun.* 71 (2006) 279; (b) M. Lamač, I. Císařová, P. Štěpnička, *Eur. J. Inorg. Chem.* (2007) 2274; (c) M. Lamač, I. Císařová, P. Štěpnička, *Collect. Czech. Chem. Commun.* 72 (2007) 985; (d) J. Kühnert, M. Lamač, T. Ruffler, B. Walfort, P. Štěpnička, H. Lang, *J. Organomet. Chem.* 692 (2007) 4303; (e) C. Bianchini, A. Meli, W. Oberhauser, A.M. Segarra, E. Passaglia, M. Lamač, P. Štěpnička, *Eur. J. Inorg. Chem.* (2008) 441; (f) M. Lamač, J. Cvačka, P. Štěpnička, *J. Organomet. Chem.* 693 (2008) 3430.
- [8] (a) This was demonstrated for alkali and alkali earth metals salts of Hdppf: (a) J. Podlaha, P. Štěpnička, I. Císařová, J. Ludvík, *Organometallics* 15 (1996) 543; (b) P. Štěpnička, J. Podlaha, *Inorg. Chem. Commun.* 1 (1998) 332.
- [9] D. Drahoňovský, I. Císařová, P. Štěpnička, H. Dvořáková, P. Maloň, D. Dvořák, *Collect. Czech. Chem. Commun.* 66 (2001) 588.
- [10] L. Meca, D. Dvořák, J. Ludvík, I. Císařová, P. Štěpnička, *Organometallics* 23 (2004) 2541.
- [11] (a) J. Kühnert, M. Dušek, J. Demel, H. Lang, P. Štěpnička, *Dalton Trans.* (2007) 2802; (b) J. Kühnert, I. Císařová, M. Lamač, P. Štěpnička, *Dalton Trans.* (2008) 2454.
- [12] (a) P. Štěpnička, J. Schulz, I. Císařová, K. Fejfarová, *Collect. Czech. Chem. Commun.* 72 (2007) 453; (b) J. Kühnert, M. Lamač, J. Demel, A. Nicolai, H. Lang, P. Štěpnička, *J. Mol. Catal. A: Chem.* 285 (2008) 4.
- [13] (a) M. Lamač, J. Tauchman, I. Císařová, P. Štěpnička, *Organometallics* 26 (2007) 5042; (b) M. Lamač, I. Císařová, P. Štěpnička, *New J. Chem.* (2009), doi:10.1039/6901262a; (c) See also: W. Zhang, T. Shimanuki, T. Kida, Y. Nakatsuji, I. Ikeda, *J. Org. Chem.* 64 (1999) 6247; (d) S.-L. You, X.-L. Hou, L.-X. Dai, B.-X. Dao, J. Sun, *Chem. Commun.* (2000) 1933; (e) J.M. Longmire, B. Wang, X. Zhang, *Tetrahedron Lett.* 41 (2000) 5435; (f) S.-L. You, X.-L. Hou, L.-X. Dai, *J. Organomet. Chem.* 637–639 (2001) 762; (g) J.M. Longmire, B. Wang, X. Zhang, *J. Am. Chem. Soc.* 124 (2002) 13400; (h) M. Tsukazaki, M. Tinkl, A. Roglans, B.J. Chapell, N.J. Taylor, V. Snieckus, *J. Am. Chem. Soc.* 118 (1996) 685; (i) R.S. Laufer, U. Veith, N.J. Taylor, V. Snieckus, *Org. Lett.* 2 (2000) 629; (j) C. Metallinos, H. Szillat, N.J. Taylor, V. Snieckus, *Adv. Synth. Catal.* 345 (2003) 370.
- [14] This method is typically used in the preparation of ferrocene conjugates with amino acids and peptides: (a) H.-B. Kraatz, *J. Inorg. Organomet. Polym. Mater.* 15 (2005) 83; (b) N. Metzler-Nolte, M. Salmann, *The bioorganometallic chemistry of ferrocene*, in: P. Štěpnička (Ed.), *Ferrocenes: Ligands, Materials and Biomolecules*, Wiley, Chichester, 2008, pp. 499–639 (Chapter 13); (c) For examples involving phosphanyl-ferrocenecarboxylic acids, see Refs. [7b], [10–12], and [13a].
- [15] W. Zhang, Y. Yoneda, T. Kida, Y. Nakatsuji, I. Ikeda, *Tetrahedron: Asymmetry* 9 (1998) 3371.
- [16] P. Štěpnička, J. Podlaha, R. Gyepes, M. Poláček, *J. Organomet. Chem.* 552 (1998) 301.
- [17] P. Štěpnička, I. Císařová, R. Gyepes, *Eur. J. Inorg. Chem.* (2006) 926.
- [18] P. Štěpnička, I. Císařová, *Collect. Czech. Chem. Commun.* 71 (2006) 215.
- [19] R.J. Coyle, Y.L. Slovokhotov, M.Y. Antipin, V.V. Grushin, *Polyhedron* 17 (1998) 3059.
- [20] V.C. Gibson, N.J. Long, A.J.P. White, C.K. Williams, D.J. Williams, M. Fontani, P. Zanello, *J. Chem. Soc., Dalton Trans.* (2002) 3280.
- [21] (a) N. Miyaura, *Metal-catalyzed cross-coupling reactions of organoboron compounds with organic halides*, in: A. de Meijere, F. Diederich (Eds.), *Metal-catalyzed Cross-Coupling Reactions*, vol. 1, Wiley-VCH, Weinheim, 2004, pp. 41–123 (Chapter 2); (b) N. Miyaura, A. Suzuki, *Chem. Rev.* 95 (1995) 2457; (c) A. Suzuki, *J. Organomet. Chem.* 576 (1999) 147; (d) N. Miyaura, *Top. Curr. Chem.* 219 (2002) 11.
- [22] (a) K.H. Shaughnessy, R.B. DeVasher, *Curr. Org. Chem.* 9 (2005) 585; (b) C.-J. Li, *Chem. Rev.* 105 (2005) 3095; (c) R. Franzén, Y. Xu, *Can. J. Chem.* 83 (2005) 266; (d) K.H. Shaughnessy, *Eur. J. Org. Chem.* (2006) 1827.
- [23] A.F. Littke, G.C. Fu, *Angew. Chem., Int. Ed.* 41 (2002) 4176.
- [24] Selected examples: (a) A.L. Casalnuovo, J.C. Calabrese, *J. Am. Chem. Soc.* 112 (1990) 4324; (b) J.P. Genet, A. Linquist, E. Blart, V. Mouriès, M. Savignac, M. Vaultier, *Tetrahedron Lett.* 36 (1995) 1443; (c) C. Dupuis, K. Adiey, L. Charrault, V. Michelet, M. Savignac, J.P. Genet, *Tetrahedron Lett.* 42 (2001) 6523; (d) L.R. Moore, K.H. Shaughnessy, *Org. Lett.* 6 (2004) 225; (e) L.R. Moore, E.C. Western, R. Craciun, J.M. Spruell, D.A. Dixon, K.P. O'Halloran, K.H. Shaughnessy, *Organometallics* 27 (2008) 576.
- [25] Selected examples: (a) K.H. Shaughnessy, R.S. Booth, *Org. Lett.* 3 (2001) 2757; (b) R.B. DeVasher, L.R. Moore, K.H. Shaughnessy, *J. Org. Chem.* 69 (2004) 7919.
- [26] H. Hattori, K. Fujita, T. Muraki, A. Sakaba, *Tetrahedron Lett.* 48 (2007) 6817.
- [27] Selected references: (a) M. Nishimura, M. Ueda, N. Miyaura, *Tetrahedron* 58 (2002) 5779; (b) K.W. Anderson, S.L. Buchwald, *Angew. Chem., Int. Ed.* 44 (2005) 6173; (c) A. Konovets, A. Penciu, E. Framery, N. Percina, C. Goux-Henry, D. Sinou, *Tetrahedron Lett.* 46 (2005) 3205.
- [28] (a) (toluene–ethanol–water + phase transfer catalyst) E. Paetzold, G. Oehme, *J. Mol. Catal. A: Chem.* 152 (2000) 69; (b) (CH₂Cl₂–water)P. Machnitzki, M. Tepper, K. Wenz, O. Stelzer, E. Herdtweck, *J. Organomet. Chem.* 602 (2000) 158; (c) (water)R.B. Bedford, M.E. Blake, C.P. Butts, D. Holder, *Chem. Commun.* (2003) 466; (d) (water)Y. Han, V. Huynh, G.K. Tan, *Organometallics* 26 (2007) 6581; (e) (THF–water)C.-P. Chang, Y.-L. Huang, F.-E. Hong, *Tetrahedron* 61 (2005) 3835; (f) (water and toluene–water)A. Buchard, B. Komly, A. Auffrant, X.G. Le Goff, P. Le Floch, *Organometallics* 27 (2008) 4380; (g) (water + phase transfer catalyst)J. Ma, X. Cui, L. Gao, Y. Wu, *Inorg. Chem. Commun.* 10 (2007) 762; (h) (water)O. Adidou, C. Goux-Henry, M. Safi, M. Soufiaoui, E. Framery, *Tetrahedron Lett.* 48 (2008) 7217; (i) (water)S.-Q. Bai, T.S.A. Hor, *Chem. Commun.* (2008) 3172.
- [29] A.O. King, N. Yasuda, *Top. Organomet. Chem.* 6 (2004) 205.
- [30] Selected examples (the product is indicated): (a) S.W. Wright, D.L. Hageman, L.D. McClure, *J. Org. Chem.* 59 (1994) 6095 (12b); (b) D. Gala, A. Stamford, J. Jenkins, M. Kugelman, *Org. Proc. Res. Dev.* 1 (1997) 163 (12a); (c) N.A. Bumagin, V.V. Bykov, *Tetrahedron* 53 (1997) 14437 (10a); (d) D.A. Alonso, C. Nájera, C. Pacheco, *J. Org. Chem.* 67 (2002) 5588 (12a); (e) C. Nájera, J. Gil-Moltó, S. Karlström, *Adv. Synth. Catal.* 346 (2004) 1798 (12a); (f) C.C. Tzschucke, W. Bannwarth, *Helv. Chim. Acta* 87 (2004) 2882 (12a); (g) C. Baleizão, A. Corma, H. Taciá, A. Leyva, *J. Org. Chem.* 69 (2004) 439; (h) O. Vassilyev, J. Chen, A.P. Panarello, J.G. Khinast, *Tetrahedron Lett.* 46 (2005) 6856 (12a); (i) G. Lu, R. Franzén, Q. Zhang, Y. Xu, *Tetrahedron Lett.* 46 (2005) 4255 (10a, 12a); (j) X. Jiang, H. Sclafani, K. Prasad, O. Repič, T.J. Blacklock, *Org. Proc. Res. Develop.* 11 (2007) 769 (12a).
- [31] (a) S.W. Chien, T.S.A. Hor, *The coordination homogeneous catalytic chemistry of 1,1-bis(diphenylphosphino)ferrocene and its chalcogenide derivatives*, in: P. Štěpnička (Ed.), *Ferrocenes: Ligands, Materials and Biomolecules*, Wiley, Chichester, 2008, pp. 33–116 (Chapter 2); (b) K.-S. Gan, T.S.A. Hor, *1,1-Bis(diphenylphosphino)ferrocene – coordination chemistry, organic syntheses, and catalysis*, in: A. Togni, T. Hayashi (Eds.), *Ferrocenes: Homogeneous Catalysis, Organic Synthesis, Materials Science, VCH, Weinheim*, 1995, pp. 3–104 (Chapter 1); (c) T.J. Colacot, S. Parisel, *Synthesis coordination chemistry and catalytic use of dpfp analogs*, in: P. Štěpnička (Ed.), *Ferrocenes: Ligands, Materials and Biomolecules*, Wiley, Chichester, 2008, pp. 117–140 (Chapter 3); (d) N. Jiang, A.J. Ragsaukas, *Tetrahedron Lett.* 47 (2006) 197.
- [32] (a) D. Braga, M. Curzi, S.L. Giuffreda, F. Grepioni, L. Maini, A. Petersen, M. Polito, *Crystal engineering with ferrocene compounds*, in: P. Štěpnička (Ed.), *Ferrocenes: Ligands, Materials and Biomolecules*, Wiley, Chichester, 2008, pp. 465–498 (Chapter 12); (b) D. Braga, *Chem. Commun.* (2003) 2751; (c) D. Braga, F. Grepioni, G.R. Desiraju, *Chem. Rev.* 98 (1998) 1375.
- [33] D. Drew, J.R. Doyle, *Inorg. Synth.* 13 (1972) 47.
- [34] J.A. Mikroyannidis, I.K. Spiliopoulos, *Polym. Sci., Part A: Polym. Chem.* 42 (2004) 1768.

- [35] N. Sakai, T. Moriya, T. Konakahara, *J. Org. Chem.* 72 (2007) 5920.
- [36] A.R. Karitzky, D. Toader, L. Xie, *Synthesis* (1996) 1425.
- [37] J. Zhao, R.C. Larock, *J. Org. Chem.* 72 (2007) 583.
- [38] (a) A. Costa, C. Nájera, J.M. Sansano, *J. Org. Chem.* 67 (2002) 5216;
(b) S. Crosignani, J. Gonzales, D. Swinnen, *Org. Lett.* 6 (2004) 4579.
- [39] Z. Otwinowski, W. Minor, *HKL DENZO AND SCALEPACK Program Package*, Nonius BV, Delft, The Netherlands. For a reference, see: Z. Otwinowski, W. Minor, *Meth. Enzymol.* 276 (1997) 307.
- [40] A. Altomare, M.C. Burla, M. Camalli, G.L. Cascarano, C. Giacovazzo, A. Guagliardi, A.G.G. Moliterni, G. Polidori, R. Spagna, *J. Appl. Crystallogr.* 32 (1999) 115.
- [41] G.M. Sheldrick, *SHELXL97*. Program for Crystal Structure Refinement from Diffraction Data, University of Goettingen, Germany, 1997.
- [42] A. L. Spek, *Platon*—a multipurpose crystallographic tool, Utrecht University, Utrecht, The Netherlands, 2003 and updates. <http://www.cryst.chem.uu.nl/platon/>. For a reference, see: A. L. Spek, *J. Appl. Cryst.* 36 (2003) 7.